J Mater Sci (2014) 49:5199–5207
DOI 10.1007/s10853-014-8229-9

Microwave-absorbing properties of silver nanoparticle/carbon nanotube hybrid nanocomposites

Gan Jet Hong Melvin · Qing-Qing Ni · Yusuke Suzuki · Toshiaki Natsuki

Received: 28 November 2013 / Accepted: 5 April 2014 / Published online: 23 April 2014

Abstract Silver (Ag) nanoparticles fabricated by chemical reduction process were grafted onto the surface of carbon nanotubes (CNTs) to prepare hybrid nanocomposites. The Ag/CNT hybrid nanomaterials were characterized using transmission electron microscopy, X-ray photoelectron spectroscopy, and Raman spectroscopy. The Ag/CNT hybrid nanomaterials were then loaded in paraffin wax, and pressed into toroidal shape with thickness of 1 mm to evaluate their complex permittivity and complex permeability by scattering parameters measurement method in reflection mode using vector network analyzer. The reflection loss of the samples was calculated according to the transmission line theory using their measured complex permittivity and permeability. The minimum reflection loss of the Ag/CNT hybrid nanocomposite sample with a thickness of 1 mm reached 21.9 dB (over 99 % absorption) at 12.9 GHz, and also exhibited a wide response bandwidth where the frequency bandwidth of the reflection loss of less than −10 dB (over 90 % absorption) was from 11.7 to 14.0 GHz. The Ag/CNT hybrid nanocomposite with thickness of 6 mm showed a minimum reflection loss of ~−32.1 dB (over 99.9 % absorption) at 3.0 GHz and was the best absorber when compared with the other samples of different thickness. The reflection loss shifted to lower frequency as the thickness of the samples increased. The capability to modulate the absorption band of these samples to suit various applications in different frequency bands simply by manipulating their thickness indicates that these hybrid nanocomposites could be a promising microwave absorber.

Keywords Microwave absorber · Silver nanoparticles · Carbon nanotubes · Reflection loss

Introduction

The advancement of electronic devices and communication instruments in commercial, industrial, scientific, and military fields, such as mobile phones, computers, radar technology, and wireless network systems is progressing rapidly [1–4]. Although these technologies are convenient, electromagnetic (EM) radiation has restricted their development and is becoming a serious problem. EM radiation can pollute the environment and harm the health of human beings, especially expectant mothers and children [1–4]. Therefore, it is essential to protect electronic devices and human beings from excessive exposure to EM radiation. Microwave-absorbing materials have received much attention to effectively solve the problem of exposure to EM radiation. An ideal microwave absorber should be lightweight, strongly absorb microwaves, and possess tunable absorption frequency, and multifunctionality [1, 2].

G. J. H. Melvin
Interdisciplinary Graduate School of Science and Technology, Shinshu University, Tokida, Ueda 386-8576, Japan

Q.-Q. Ni (✉) · T. Natsuki
Department of Functional Machinery and Mechanics, Shinshu University, Tokida, Ueda 386-8576, Japan
e-mail: niqq@shinshu-u.ac.jp

Q.-Q. Ni
Key Laboratory of Advanced Textile Materials and Manufacturing Technology, Ministry of Education, Zhejiang Sci-Tech University, Hangzhou, China

Y. Suzuki
Graduate School of Science and Technology, Shinshu University, Tokida, Ueda 386-8576, Japan

Nanomaterials such as nanoparticles and nanocomposites are among important candidates as microwave-absorbing materials [5]. The relative density of nanomaterials is lower and their specific surface area is larger than those of the corresponding bulk materials. As a result, there are a large number of active atoms at the nanomaterial surface, which has a large interfacial dielectric loss induced by interface polarization [1]. Metal nanoparticles such as silver (Ag) nanoparticles hybridized with carbon nanotubes (CNTs) have potential to be developed as advanced materials for a wide range of applications [6–11], including as microwave-absorbing materials [12, 13]. CNTs are light, possess a high aspect ratio and unique magnetic properties, and exhibit favorable mechanical, chemical, and electric properties that have attracted considerable attention [2, 7–9, 13–16]. Their high electrical conductivity makes CNTs capable of dissipating electrostatic charges or shielding EM radiation [16]. However, CNTs disperse poorly in organic and aqueous solvents because of a strong intrinsic van der Waals attraction [11, 17]. Many techniques have been used to solve the problem by functionalizing the CNTs using acid treatment [12, 13, 18], mild hydrothermal treatment [17], microwave-induced radical polymerization [19], and so on. In this study, we used acid treatment method to functionalize the CNTs. This treatment is fast, easy, and leads to the introduction of carboxyl and hydroxyl groups to the surface of the CNTs, which allows them to be highly dispersed in polar solvents. Furthermore, Ag is a good conductor, abundant, easy to prepare, and inexpensive [9–11]. Ag nanoparticles decoration would have a beneficial effect on the electrical conductivity of CNTs because the inherent electrical conductivity of Ag is superior to the CNTs without Ag [9]. Metal nanoparticles such as Ag nanoparticles, produced large electric or magnetic loss and have been demonstrated to show promising microwave absorption [1, 4]. Furthermore, metal nanoparticles such as Ag nanoparticles decorated on the CNTs will absorb the microwave energy through electrons hopping and shows enhanced microwave absorption bandwidth [2]. The combination of Ag nanoparticles with CNTs can integrate the properties of these two components to form hybrid nanocomposites for use as microwave-absorbing materials.

Reports on Ag nanoparticles or Ag/CNT hybrid materials as microwave absorbers are very limited. Ramesh et al. [4] investigated the microwave-absorbing properties of Ag nanoparticles embedded in thin polymer films. Meanwhile, Zhao et al. [12, 13] investigated the microwave-absorbing properties of CNTs filled with Ag nanowires. To the best of our knowledge, the microwave-absorbing properties of Ag/CNT hybrid nanocomposites where Ag nanoparticles are decorated on the surface of CNTs have not been examined.

In this study, we prepare Ag nanoparticles and graft them onto the surface of CNTs. We then evaluate the ability of these materials to absorb microwaves by measuring their dielectric and/or magnetic losses when penetrated by an EM wave [1, 16]. The complex permittivity and complex permeability of these hybrid nanocomposites are measured, and their reflection loss is also evaluated.

Experimental

Modification of CNTs

CNTs can be modified with a single or mixture of acids [12, 13, 18]. Multi-walled CNTs (Wako Pure Chemical Industries Ltd., Japan, $d = 40$–70 nm) were functionalized by chemical oxidation in nitric acid (HNO_3). The CNTs were heated under reflux in boiling HNO_3 at 120 °C for 10 h. The resulting mixture was centrifuged with pure water, diluted with pure water, and left overnight until the pH was neutral. The CNTs were centrifuged again with pure water to separate them, and then dried overnight at 60 °C. The acid-treated CNTs are denoted as modified CNTs hereafter. The samples for pristine CNTs were prepared by using obtained CNTs without any further modification.

Preparation of Ag nanoparticles

Ag nanoparticles can be produced by chemical reduction, which only requires simple equipment and is convenient, inexpensive, and gives a high yield [18, 20, 21]. The preparation is based on Ref. [20, 21], where method in Ref. [20] was done by one of our research group. This method has advantages including short reaction time; small and relatively uniform particles can be fabricated; the reaction proceeds rapidly at room temperature; high purity and good conductivity. Silver nitrate ($AgNO_3$), sodium citrate (Na_3Ct), and 2-dimethylaminoethanol (DMAE) were obtained from Wako Pure Chemical Industries Ltd., Japan. Polyvinylpyrrolidone (PVP, K 15, Tokyo Chemical Industry Co. Ltd., Japan) was used to prevent aggregation of the Ag nanoparticles.

PVP (1.0 g) was stirred in pure water (20 mL) for 10 min. $AgNO_3$ (0.5 g) was added, and the mixture was stirred vigorously for 10 min. Na_3Ct (0.88 g) diluted in pure water (20 mL) was added dropwise to the stirred mixture. Then, DMAE (0.03 g) was added and the mixture was stirred for 1 h. Finally, the mixture was centrifuged, washed with pure water, and dispersed in ethanol (10 mL). The Ag nanoparticles dispersed in ethanol (solution A) were used to prepare Ag/CNT hybrid nanocomposites.

Preparation of Ag/CNT hybrid nanocomposites

Ag nanoparticles were grafted onto the surface of the CNTs according to the method reported in Ref. [18] with some modification. Cysteamine hydrochloride and 2,5-dihydroxybenzoic acid (DHB) obtained from Wako Pure Chemical Industries Ltd., Japan, were used to link the Ag nanoparticles to the surface of the CNTs.

Ag nanoparticles in ethanol (5 mL, obtained from solution A) were sonicated for 10 min, and then reacted with cysteamine hydrochloride (0.23 g) in ethanol (95 mL) at 80 °C for 6 h in an oil bath (mixture A). The total volume of mixture A was 100 mL. At the same time, modified CNTs (0.05 g) were sonicated in ethanol (100 mL) for 1 h (mixture B). DHB (0.08 g) was added to mixture B, which was then sonicated for 30 min. Mixture A and B were combined, and then stirred for 24 h. The resulting product was centrifuged, washed with pure water, and then dried overnight at 60 °C.

Evaluation methods

Transmission electron microscopy (TEM) images of the Ag nanoparticles, modified CNTs, and Ag/CNT hybrid nanomaterials were obtained using a TEM (JEM-2100, JOEL, Japan) with an accelerating voltage of 200 kV. X-ray photoelectron spectroscopy (XPS, Kratos Axis Ultra DLD) was performed with a standard Mg Kα (1256.6 eV) X-ray source operating at 10 mA and 15 kV to characterize the elemental composition and chemical states of the samples. Raman spectroscopy measurements were performed on a Raman spectrometer (HoloLab series 5000, Kaiser Optical Systems) with 532-nm laser excitation.

The real and imaginary parts of complex permittivity ε ($\varepsilon = \varepsilon' - j\varepsilon''$) and permeability μ ($\mu = \mu' - j\mu''$) were measured by scattering parameters measurement method in reflection mode using a vector network analyzer (37247D, Anritsu Co. Ltd.) within the frequency range of 0.5–14 GHz. Samples for these measurements were prepared by loading the Ag/CNT hybrid nanocomposites in paraffin wax with a weight percentage of Ag/CNT hybrid nanocomposite to paraffin of 30 %. The complex permittivity and permeability of the paraffin wax are low and constant throughout the frequency range [12]. Furthermore, the paraffin wax shows almost no absorption. The powder-wax composites were pressed into a toroidal shape using a mold designed with an outer diameter of 7 mm, inner diameter of 3 mm, and thickness of 1 mm. The thickness was also measured using vernier caliper to check the uniformity. The reflection loss was calculated from the measured complex permittivity and permeability of the samples.

Results and discussion

Morphology of Ag/CNT hybrid nanocomposites

TEM images of the Ag nanoparticles, modified CNTs and Ag/CNT hybrid nanocomposites are depicted in Fig. 1. Figure 1a, b show that the Ag nanoparticles had diameters of less than 10 nm, ranging from 5 to 10 nm. Figure 1c shows the modified CNTs before Ag nanoparticles were grafted on their surfaces. The diameter of the CNTs was about 40 nm, and they contained some defects on their walls after modification by acid treatment. Figure 1d, e, f show TEM images of the Ag/CNT hybrid nanocomposites with Ag nanoparticles grafted onto the surface of the CNTs. Ag nanoparticles were homogeneously dispersed with no agglomeration and strongly adhered to the surfaces of the CNTs. The diameter of the Ag nanoparticles grafted onto the surface of the CNTs was also less than 10 nm.

XPS analysis of Ag/CNT hybrid nanocomposites

XPS evaluation was carried out to determine the elemental composition and functional groups of the pristine CNTs, modified CNTs, and Ag/CNT hybrid nanocomposites, as shown in Fig. 2. The pristine and modified CNTs exhibited a strong carbon (C 1s) peak at 284 eV and oxygen (O 1s) peak at 532 eV. The modified CNTs clearly showed an O 1s peak with higher intensity than that of the pristine CNTs. The atomic percentage ratios for the pristine CNTs are 98.59 % for C 1s and 1.41 % for O 1s, while those of the modified CNTs are 92.40 % for C 1s and 7.60 % for O 1s. The higher intensity of the O 1s peak confirms that many oxygen functional groups (carboxyl and hydroxyl) were introduced onto the surface of the CNTs modified by acid treatment.

The XPS survey spectrum of the Ag/CNT hybrid nanomaterial confirmed the presence of C 1s, O 1s, nitrogen (N 1s), chlorine (Cl $2p_{3/2}$), silver (Ag 3d, Ag 3p), and sulfur (S 2s, S 2p). The Ag/CNT samples showed a strong C 1s peak at 284 eV, O 1s peak at 531 eV, N 1s peak at 400 eV, and Cl $2p_{3/2}$ peak at 198 eV. Ag 3d peaks from Ag $3d_{5/2}$ and Ag $3d_{3/2}$ appeared at 368 and 374 eV, respectively. Ag 3p peaks from Ag $3p_{3/2}$ and Ag $3p_{1/2}$ were observed at 573 and 604 eV, respectively. The S 2s and S 2p peaks appeared at 227 and 163 eV, respectively. The presence of Ag 3d and Ag 3p peaks proves the formation of Ag nanoparticles. Furthermore, the observation of N 1s, Cl $2p_{3/2}$, S 2s, S 2p, Ag 3d, and Ag 3p peaks confirmed that the amidation reaction between cysteamine hydrochloride ($NH_2(CH_2)_2SH{\cdot}HCl$) and Ag nanoparticles was successful [18]. The CNTs were oxidized using acid treatment in order to introduce carboxyl and hydroxyl groups onto the

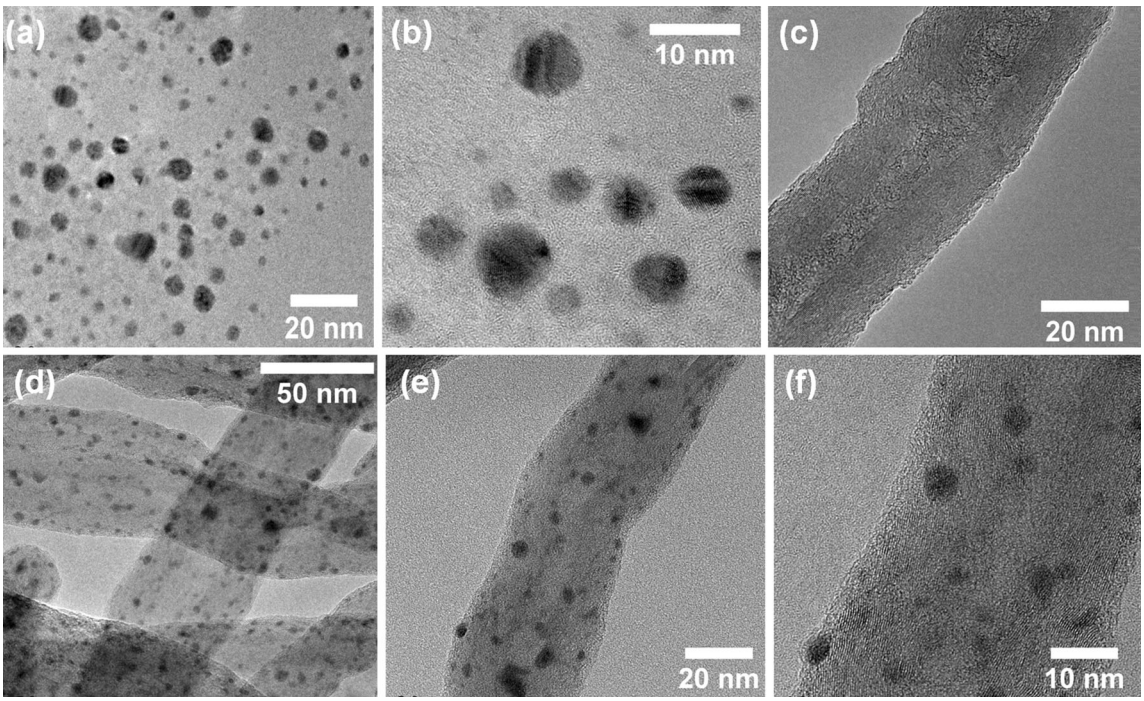

Fig. 1 TEM images of **a**, **b** Ag nanoparticles; **c** modified CNTs; **d**, **e**, and **f** Ag/CNT hybrid nanocomposites

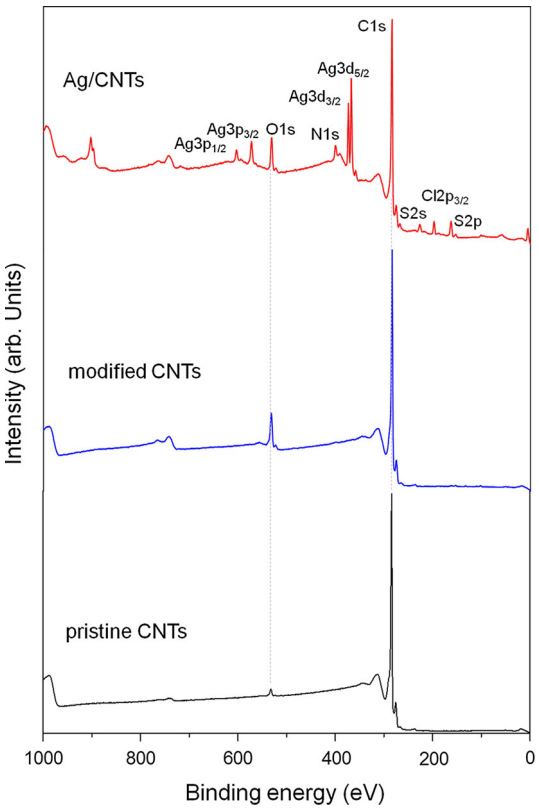

Fig. 2 XPS spectra of pristine CNTs, modified CNTs, and Ag/CNT hybrid nanocomposites

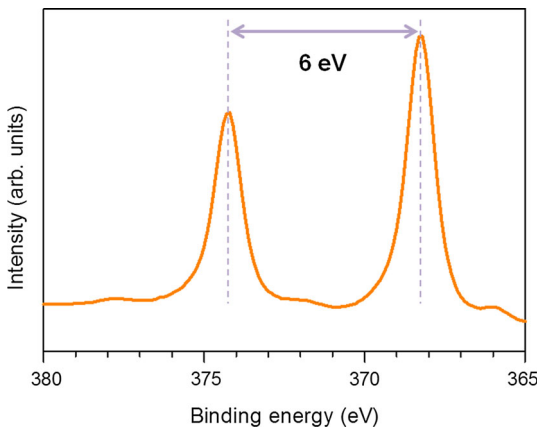

Fig. 3 XPS of the Ag 3d core level of the Ag/CNT hybrid nanocomposites

surface of CNTs. Ag nanoparticles were modified with self-assembled monolayers cysteamine hydrochloride, resulting in cysteamine hydrochloride-Ag groups. Using DHB as a coupling agent, the modified CNTs functionalized with carboxyl and hydroxyl groups on the surface reacted with the amino groups on the silver surface through amide bonds [18]. The Ag 3d doublet peaks with separation energy of 6 eV shown in Fig. 3 are consistent with Ag metal, further confirming that Ag on the surface of the

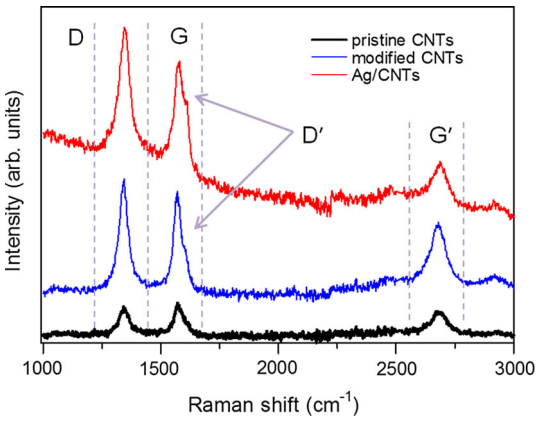

Fig. 4 Raman spectra of pristine CNTs, modified CNTs, and Ag/CNT hybrid nanocomposites

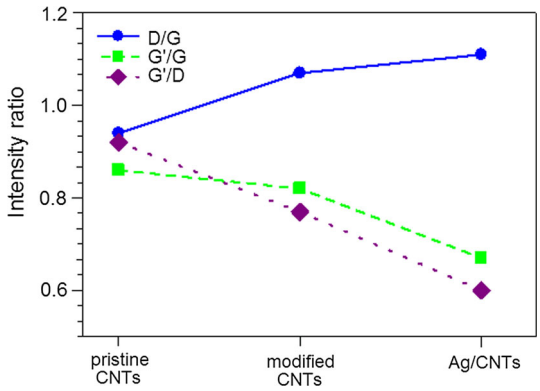

Fig. 5 Relative intensity ratios of D/G, G′/G, and G′/D peaks of pristine CNTs, modified CNTs, and Ag/CNT hybrid nanocomposites

CNTs exists in the zero-valent state [7, 8, 18]. The atomic percentage ratios for the Ag/CNT nanomaterials are 87.02 % for C 1s, 7.04 % for O 1s, 2.73 % for Ag 3d, and 3.22 % for Ag 3p.

Raman spectroscopy of Ag/CNT hybrid nanocomposites

Raman spectroscopy is an effective tool to characterize carbon-based materials [17, 19, 22–24], so Raman spectra of the pristine CNTs, modified CNTs, and Ag/CNT hybrid nanocomposites were measured. The characteristic bands of CNTs, D band (defect) at $\sim$1350 cm^{-1}, G band (graphite band) at $\sim$1580 cm^{-1}, and G′ band (D overtone) at $\sim$2700 cm^{-1} were observed, as illustrated in Fig. 4. The D′ band of the modified CNTs and Ag/CNT hybrid nanocomposites ranging from 1600 to 1620 cm^{-1}, which is attributed to structural defects and broadened caused by modification with Ag [24], was also observed. For the Ag/CNT hybrid nanocomposites, the G′ peak shifted to higher wavenumber, $\sim$2688 cm^{-1} (pristine CNTs: $\sim$2679 cm^{-1}, modified CNTs: $\sim$2680 cm^{-1}), because of a substantial charge transfer interaction between the Ag nanoparticles and CNTs [24].

The relative intensity of the D and G bands (I_D/I_G) is related to the amount of structural defects and sp^3-hybridized carbon atoms in a CNT sample, and thus provides direct information about the degree of sidewall functionalization [19, 22]. Furthermore, the relative intensity of the G′ and G bands ($I_{G'}/I_G$) and the relative intensity of the G′ and D bands ($I_{G'}/I_D$), which are related to the scale on which the graphitic order extends and the degree of crystallinity [22], respectively, were also evaluated. The relative intensities of the D/G, G′/G, and G′/D ratios are presented in Fig. 5. The D/G ratio is 0.94, 1.07, and 1.11 for the pristine CNTs, modified CNTs, and Ag/CNT hybrid nanocomposites, respectively. The increase of the D/G ratio of the modified CNTs compared with that of the pristine CNTs confirms the successful introduction of functional groups onto the CNTs surface and that the outer layers of the CNTs were chemically modified [17, 19]. The slight increase between the D/G ratio of the modified CNTs and that of the Ag/CNT hybrid nanocomposites can be attributed to the introduction of Ag nanoparticles onto the surface of the CNTs. The G′/G ratio is 0.86, 0.82, and 0.67 for the pristine CNTs, modified CNTs, and Ag/CNT hybrid nanocomposites, respectively. Moreover, the G′/D ratio is 0.92, 0.77, and 0.60 for the pristine CNTs, modified CNTs, and Ag/CNT hybrid nanocomposites, respectively. The decrease of the G′/G and G′/D ratios of the modified CNTs compared with those of the pristine CNTs reveals a higher density of lattice defects in the acid-treated CNTs [22]. A decrease of the intensity of the G′ peak of the Ag/CNT hybrid nanocomposites (Fig. 4) as the mass fraction of CNTs in the hybrid material decreases is also clear. The G′ peak arises from a two-phonon process, so it is reasonable that its intensity decreases as the sample becomes less ordered (i.e., more impurities or introduced surface species), not allowing for the coupling effect that is required for the two-phonon process [25]. The G′/G and G′/D ratios of the Ag/CNT hybrid nanocomposites showed the lowest values because the CNTs were sonicated before being attached with Ag nanoparticles, which promotes the formation of structural defects. Attachment of Ag nanoparticles could also cause the G′/G and G′/D ratios to decrease through the interaction between the Ag nanoparticles and CNTs.

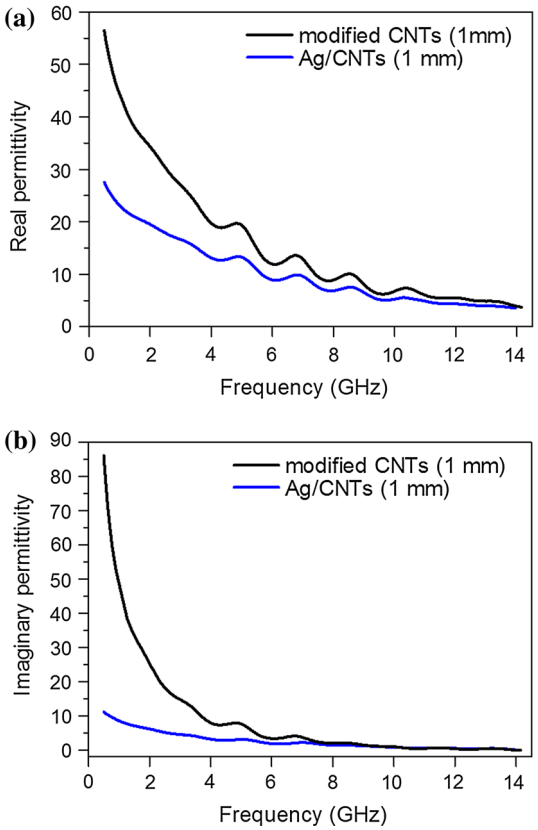

Fig. 6 Complex permittivity of the modified CNT composite ($t = 1$ mm) and Ag/CNT hybrid nanocomposite ($t = 1$ mm). **a** Real part permittivity, and **b** imaginary part permittivity

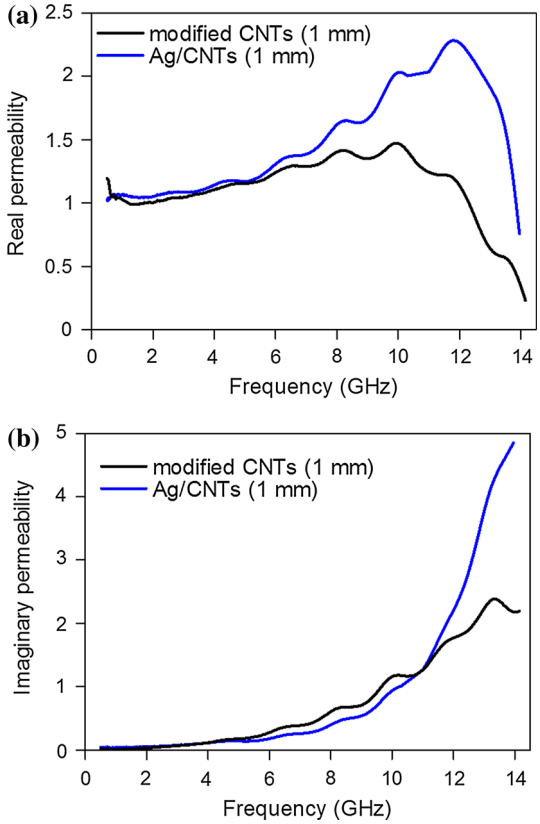

Fig. 7 Complex permeability of the modified CNT composite ($t = 1$ mm) and Ag/CNT hybrid nanocomposite ($t = 1$ mm). **a** Real part permeability, and **b** imaginary part permeability

Electromagnetic wave absorption properties

Complex permittivity and complex permeability are basic parameters associated with the microwave absorption properties of a material, where the real parts of complex permittivity and permeability represent the storage of electric and magnetic energies, respectively, while the imaginary parts symbolize the loss and dissipation of both energies [1, 2]. The complex permittivity (real part ε' and imaginary part ε'') of the modified CNT composite (thickness, $t = 1$ mm) and Ag/CNT composite ($t = 1$ mm) loaded in paraffin wax in the range of 0.5–14 GHz is presented in Fig. 6. As the frequency increased, the complex permittivity decreased because the polarizabilities (electronic, ionic, and orientation) and electric displacement are not maintained in a changing EM field [26, 27]. The modified CNTs composite exhibited higher complex permittivity than the Ag/CNT hybrid nanocomposite. This can be explained by the high electrical conductivity of the CNTs that enables strong polarization to occur, Ohmic losses, dissipation of electrostatic charges, or multiple scattering caused by the large specific area, which lead to improved complex permittivity [2, 16]. The behavior of the complex permittivity of the Ag/CNT hybrid nanocomposites can be attributed to the multiple interfacial polarizations between the Ag nanoparticles, CNTs, and paraffin wax [27]. Furthermore, the polarization mainly contains thermal ion polarization, dipole rotation polarization, electronic displacement polarization, ion polarization, and so on [1]. The time for electronic displacement and ion polarization is very short, thus these polarizations produce energy loss at high frequency region [1].

The complex permeability (real part μ', imaginary part μ'') of the modified CNTs composite ($t = 1$ mm) and Ag/CNT hybrid nanocomposite ($t = 1$ mm) in the range of 0.5–14 GHz is shown in Fig. 7. Interestingly, the presence of Ag nanoparticles affected the complex permeability of the hybrid nanocomposites. μ' of the Ag/CNT hybrid nanocomposite was higher than that of the modified CNT composite, and increased until a certain frequency, after which it gradually decreased. This can be attributed to natural resonance or eddy current loss [1, 27]. When Ag (conducting material) was put in an alternating magnetic field, a close induced current will be produced inside the material, which would dissipate the energy and referred as eddy current loss [1]. Both Ag and CNTs possess

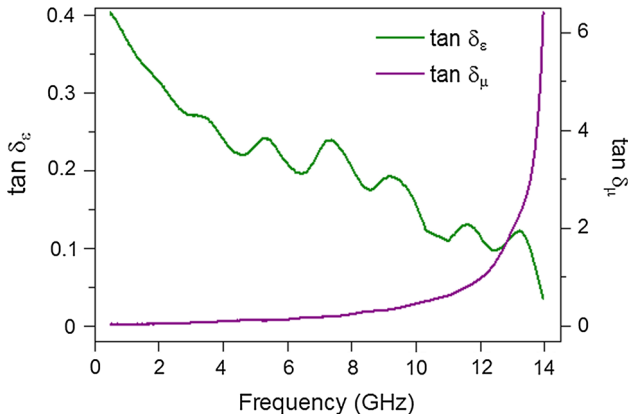

Fig. 8 Dielectric loss factor and magnetic loss factor of the Ag/CNT hybrid nanocomposite with $t = 1$ mm

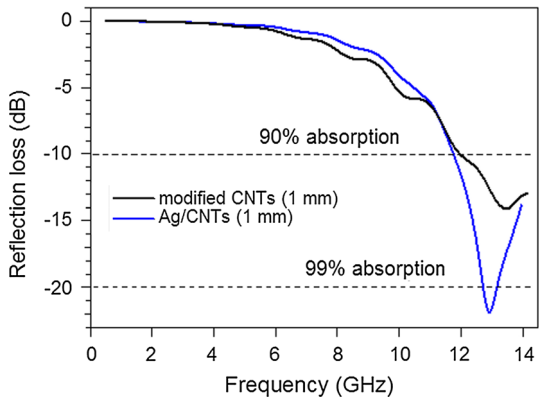

Fig. 9 Reflection loss of the modified CNT composite ($t = 1$ mm) and Ag/CNT hybrid nanocomposite ($t = 1$ mm) in the range of 0.5–14 GHz

high electrical conductivity. This leads to permeability decreasing rapidly at high frequency caused by the eddy current loss. The strong attenuation of permeability with increasing frequency is due to the screening of the electromagnetic field by eddy currents [28]. This reduces the initial permeability and introduces a typical decaying envelope in the intrinsic permeability signal [28]. When a composite is exposed to a changing EM field, the Lorentz force on the electrons in the Ag nanoparticles provokes them to circulate, producing eddy currents [27]. A magnetic field induced by the eddy currents that opposes the applied field causes the composites to radiate an EM wave, which increases the total magnetic energy and results in decreased permeability [15, 27].

To reveal the intrinsic reasons for the microwave absorption by the Ag/CNT hybrid nanocomposites, their dielectric loss factor ($\tan\delta_\varepsilon = \varepsilon''/\varepsilon'$) and magnetic loss factor ($\tan\delta_\mu = \mu''/\mu'$) were evaluated. Figure 8 presents $\tan\delta_\varepsilon$ and $\tan\delta_\mu$ of the Ag/CNT hybrid nanocomposite with $t = 1$ mm. The relaxation observed from $\tan\delta_\varepsilon$ can be attributed from energy loss in the materials illuminated by electromagnetic field comes about through damping forces acting on polarized atoms and molecules and trough the finite conductivity of the materials [2]. Both $\tan\delta_\varepsilon$ and $\tan\delta_\mu$ contribute to the microwave absorption; in the low frequency region, $\tan\delta_\varepsilon$ is sensitive to microwaves; and at high frequency, $\tan\delta_\mu$ is sensitive to microwaves.

To investigate the microwave absorption properties of the samples, the reflection loss (*R.L.*) was calculated according to the transmission line theory as follows:

$$R.L. = 20\log\left|\frac{Z_{in}-1}{Z_{in}+1}\right|, \quad (1)$$

where the normalized input impedance (Z_{in}) is given by the formula,

$$Z_{in} = \sqrt{\frac{\mu_r}{\varepsilon_r}}\tanh\left[j\left(\frac{2\pi fd}{c}\right)\sqrt{\mu_r\varepsilon_r}\right] \quad (2)$$

where $\varepsilon_r = \varepsilon' - j\varepsilon''$, $\mu_r = \mu' - j\mu''$, f is the microwave frequency (Hz), d is the thickness of the absorber (m), and c is the velocity of light in free space (m/s). *R.L.* of the modified CNT composite with $t = 1$ mm and the Ag/CNT hybrid nanocomposites with $t = 1$ mm are shown in Fig. 9.

The Ag/CNT hybrid nanocomposite with $t = 1$ mm showed a minimum *R.L.* of ~ -21.9 dB (over 99 % absorption) at 12.9 GHz. Furthermore, this sample also exhibited a wide response bandwidth of 2.3 GHz, where the frequency bandwidth (*R.L.* of less than -10 dB, over 90 % absorption) is from 11.7 to 14.0 GHz. Conversely, the modified CNT composite with $t = 1$ mm showed a minimum *R.L.* of ~ -14.1 dB at 13.5 GHz with a response bandwidth of 2.0 GHz (12.0–14.0 GHz). The peak of the minimum *R.L.* shifted to lower frequency for the Ag/CNT hybrid nanocomposite compared with that of the modified CNT composite of similar thickness. Moreover, *R.L.* and the response bandwidth of the Ag/CNT hybrid nanocomposite are both superior to the equivalent values of the modified CNT composite. Even though the modified CNT composite exhibited higher complex permittivity and complex permeability, the Ag/CNT hybrid nanocomposite was the better absorber because it showed a higher minimum *R.L.* According to Ref. [1, 2], suitable complex permittivity and complex permeability are essential to promote EM wave absorption. This also can be related to another important parameter connected to *R.L.*, i.e., the concept of matched impedance. This concept suggests that the characteristic impedance of an absorber should be almost equal to that of the free space to achieve zero reflection on the front surface of the material [29–31].

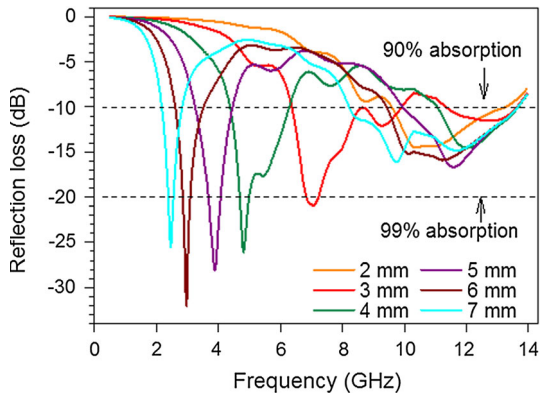

Fig. 10 Reflection loss of the Ag/CNT hybrid nanocomposite ($t = 2$, 3, 4, 5, 6, and 7 mm) in the range of 0.5–14 GHz

Obviously, to design an optimized absorber with a high minimum *R.L.*, appropriate EM impedance matching is important.

There are many boundaries in the Ag/CNT hybrid nanocomposites, including between the Ag surfaces, CNT surfaces, and paraffin wax. Moreover, because the CNTs were modified both prior to and during the process of Ag nanoparticle coating, the Ag/CNT hybrid nanocomposites contain many defects and suspended bonds, as shown in the Raman spectra of the samples (Figs. 4, 5). As a result, the large specific areas of the surfaces of the hybrid nanocomposites triggered higher interfacial polarization and multiple scattering, which leads to a high minimum *R.L.*. Interfacial multipoles contribute to the strong EM wave absorption of the hybrid nanocomposites.

According to Eq. (2), the thickness of the absorber can also affect *R.L.*, so we investigated the relationship between the thickness and *R.L.* of the Ag/CNT hybrid nanocomposites. *R.L.* for Ag/CNT hybrid nanocomposites with $t = 2$, 3, 4, 5, 6, and 7 mm was calculated and shown in Fig. 10. When the thickness of the Ag/CNT hybrid nanocomposite increased, the frequency of the *R.L.* peak decreased. When $t = 3$ mm and above, extra peak was observed at lower frequency region, between 0.5 to 9.0 GHz. The *R.L.* peaks at higher frequency showed over 90 % absorption (>10 dB) meanwhile, the *R.L.* peaks at lower frequency showed over 99 % absorption (>20 dB). As the thickness increased beyond $t = 3$ mm, the *R.L.* peak (response bandwidth) at high frequency region become broader; and *R.L.* peak at low frequency region become narrower. The Ag/CNT hybrid nanocomposite with $t = 6$ mm showed a minimum *R.L.* of ~ -32.1 dB (over 99.9 % absorption) at 3.0 GHz and was the best absorber when compared with the other samples of different thickness. Furthermore, they also showed *R.L.* of less than -10 dB, from 2.6 to 3.5 GHz (low frequency region) and 9.4 to 13.7 GHz (high frequency region), respectively. These results show that the frequency related to the minimum *R.L.* (highest absorption) of the Ag/CNT hybrid nanocomposites can be controlled by changing the thickness of the sample. Furthermore, absorption at low and high frequency region also can be archived by changing the thickness of Ag/CNT hybrid nanocomposites. We believe that the Ag/CNT hybrid nanocomposites are a promising microwave absorber, because their absorption band can be modulated simply by manipulating the sample thickness to satisfy applications in different frequency bands.

Conclusions

Ag nanoparticles were grafted onto the surface of CNTs to fabricate Ag/CNT hybrid nanomaterials. TEM, XPS, and Raman spectroscopy analyses revealed the morphology, structure, and elemental composition of the hybrid nanomaterials. The Ag nanoparticles were less than 10 nm in diameter and showed no agglomeration when adhered to the surface of CNTs. The high interfacial area of the hybrid nanomaterials results in high interfacial polarization and multiple scattering, which improves microwave absorption. The Ag/CNT hybrid nanomaterials exhibited a minimum *R.L.* of 21.9 dB (over 99 % absorption) at 12.9 GHz with a wide response bandwidth (2.3 GHz), superior than the modified CNT composite with same thickness of 1 mm. Furthermore, the Ag/CNT hybrid nanomaterials, $t = 6$ mm showed a minimum *R.L.* of ~ -32.1 dB (over 99.9 % absorption) at 3.0 GHz and was the best absorber when compared with the other samples of different thickness. The Ag/CNT hybrid nanomaterials showed two *R.L.* peaks, at low and high frequency region, as the thickness of the sample increased. They also showed wide minimum *R.L.* of over -10 dB (over 90 % absorption). This proves that the thickness of samples can be manipulated to produce absorption bands at different frequencies to design highly effective microwave absorbers.

Acknowledgements This work was supported by Grants for Excellent Graduate Schools by the Ministry of Education, Culture, Sports, Science and Technology, Japan.

References

1. Huo J, Wang L, Yu H (2009) Polymeric nanocomposites for electromagnetic wave absorption. J Mater Sci 44:3917–3927. doi:10.1007/s10853-009-3561-1
2. Qin F, Brosseau C (2012) A review and analysis of microwave absorption in polymer composites filled with carbonaceous particles. J Appl Phys 111:061301
3. Zhu HL, Bai YJ, Liu R, Lun N, Qi YX et al (2011) Microwave absorption properties of MWCNT-SiC composites synthesized via a low temperature induced reaction. AIP Adv 1:032140

4. Ramesh GV, Sudheendran K, Raju KCJ et al (2009) Microwave absorber based on silver nanoparticle-embedded polymer thin film. J Nanosci Nanotechnol 9:261–266
5. Peng CH, Wang HW, Kan SW, Shen MZ, Wei YM, Chen SY (2004) Microwave absorbing materials using Ag–NiZn ferrite core-shell nanopowders as fillers. J Magn Magn Mater 284:113–119
6. Ma PC, Tang BZ, Kim JK (2008) Effect of CNT decoration with silver nanoparticles on electrical conductivity of CNT-polymer composites. Carbon 46:1497–1505
7. Jiang Y, Lu Y, Zhang L, Liu L, Dai Y, Wang W (2012) Preparation and characterization of silver nanoparticles immobilized on multi-walled carbon nanotubes by poly (dopamine) functionalization. J Nanopart Res 14:938
8. Chen L, Xie H, Yu W (2012) Multi-walled carbon nanotube/silver nanoparticles used for thermal transportation. J Mater Sci 47:5590–5595. doi:10.1007/s10853-012-6451-x
9. Zhang W, Li W, Wang J, Qin C, Dai L (2010) Composites of polyvinyl alcohol and carbon nanotubes decorated with silver nanoparticles. Fibers Polym 11:1132–1136
10. Yang GW, Gao GY, Wang C, Xu CL, Li HL (2008) Controllable deposition of Ag nanoparticles on carbon nanotubes as a catalyst for hydrazine oxidation. Carbon 46:747–752
11. Dong RX, Liu CT, Huang KC, Chiu WY, Ho KC, Lin JJ (2012) Controlling formation of silver/carbon nanotube networks for highly conductive film surface. ACS Appl Mater Interfaces 4:1449–1455
12. Zhao DL, Li X, Shen ZM (2008) Electromagnetic and microwave absorbing properties of multi-walled carbon nanotubes filled with Ag nanowires. Mater Sci Eng B 150:105–110
13. Zhao DL, Li X, Shen ZM (2008) Microwave absorbing property and complex permittivity and permeability of epoxy composites containing Ni-coated and Ag filled carbon nanotubes. Compos Sci Technol 68:2902–2908
14. Katsounaros A, Rajab KZ, Hao Y, Mann M, Milne WI (2011) Microwave characterization of vertically aligned multiwalled carbon nanotube arrays. Appl Phys Lett 98:203105
15. Deng L, Han M (2007) Microwave absorbing performances of multiwalled carbon nanotube composites with negative permeability. Appl Phys Lett 91:023119
16. Ting TH, Jau YN, Yu RP (2012) Microwave absorbing properties of polyaniline/multi-walled carbon nanotube composites with various polyaniline contents. Appl Surf Sci 258:3184–3190
17. Zhang L, Hashimoto Y, Taishi T, Ni QQ (2011) Mild hydrothermal treatment to prepare highly dispersed multi-walled carbon nanotubes. Appl Surf Sci 257:1845–1849
18. Lee SH, Teng CC, Ma CCM, Wang I (2011) Highly transparent and conductive thin films fabricated with nano-silver/double-walled carbon nanotube composite. J Colloid Interface Sci 364:1–9
19. Zhang L, Ni QQ, Shiga A, Natsuki T, Fu Y (2011) Preparation of polybenzimidazole/functionalized carbon nanotube nanocomposite films for the use as protective coatings. Polym Eng Sci 51:1525–2532
20. Natsuki J, Natsuki T, Abe T (2013) Low molecular weight compounds as effective dispersing agents in the formation of colloidal silver nanoparticles. J Nanopart Res 15:1483
21. Natsuki J, Abe T (2011) Synthesis of pure colloidal silver nanoparticles with high electroconductivity for printed electronic circuits: The effect of amines on their formation in aqueous media. J Colloid Interface Sci 359:19–23
22. Santangelo S, Messina G, Faggio G, Lanza M, Milone C (2011) Evaluation of crystalline perfection degree of multi-walled carbon nanotubes: correlations between thermal kinetic analysis and micro-Raman spectroscopy. J Raman Spectrosc 42:593–602
23. Lin Y, Watson KA, Fallbach MJ, Ghose S et al (2009) Rapid, solventless, bulk preparation of metal nanoparticle-decorated carbon nanotubes. ACS Nano 3:871–884
24. Corio P, Santos AP, Santos PS, Temperini MLA, Brar VW et al (2004) Characterization of single wall carbon nanotubes filled with silver and with chromium compounds. Chem Phys Lett 383:475–480
25. DiLeo RA, Landi BJ, Raffaelle RP (2007) Purity assessment of multi-walled carbon nanotubes by Raman spectroscopy. J Appl Phys 101:064307
26. Wang G, Chen X, Duan Y, Liu S (2008) Electromagnetic properties of carbon black and barium titanate composite materials. J Alloys Compd 454:340–346
27. Wu H, Wang L, Wang Y, Guo S, Shen Z (2012) Enhanced microwave absorbing properties of carbonyl iron-doped Ag/ordered mesoporous carbon nanocomposites. Mater Sci Eng B 177:476–482
28. Viegas ADC, Correa MA, Santi L, da Silva RB, Bohn F, Carara M, Sommer RL (2007) Thickness dependence of the high-frequency magnetic permeability in amorphous $Fe_{73.5}Cu_1Nb_3Si_{13.5}B_9$ thin films. J Appl Phys 101:033908
29. Kim JH, Kim SS (2011) Microwave absorbing properties of Ag-coated Ni–Zn ferrite microspheres prepared by electroless pplating. J Alloys Compd 509:4399–4403
30. Cui C, Du Y, Li T, Zheng X et al (2012) Synthesis of electromagnetic functionalized Fe_3O_4 microspheres/polyaniline composites by two-step oxidative polymerization. J Phys Chem B 116:9523–9531
31. Yuchang Q, Wancheng Z, Fa L, Dongmei Z (2011) Optimization of electromagnetic matching of carbonyl iron/$BaTiO_3$ composites for microwave absorption. J Magn Magn Mater 323:600–606